Chapter 12
Imaging of Congenital Anomalies of the Kidney and Urinary Tract

Nora G. Lee, Sherry S. Ross, and H. Gil Rushton

Abbreviations

ADPKD	Autosomal dominant polycystic kidney disease
APD	Anterior–posterior diameter
ARPKD	Autosomal recessive polycystic kidney disease
CT	Computerized tomography
DMSA	Dimercaptosuccinic acid
DRF	Differential renal function
IVP	Intravenous pyelography
KUB	Abdominal plain film of kidney ureter, bladder
MCDK	Multicystic dysplastic kidney
MRI	Magnetic resonance imaging
PUV	Posterior urethral valve
RNC	Radionuclide cystography
SFU	Society for fetal urology
UPJ	Ureteropelvic junction
UTI	Urinary tract infection
VCUG	Voiding cystourethrogram
VUR	Vesicoureteral reflux

N.G. Lee, M.D.
Department of Urology, University of Virginia Health System, Charlottesville, VA, USA

S.S. Ross, M.D.
Department of Urology, The University of North Carolina at Chapel Hill, Chapel Hill, NC, USA

H. Gil Rushton, M.D. (✉)
Division of Pediatric Urology, Children's National Medical Center, Departments of Urology and Pediatrics, The George Washington University School of Medicine, Washington, DC, USA
e-mail: hrushton@cnmc.org

A.J. Barakat, H. Gil Rushton (eds.), *Congenital Anomalies of the Kidney and Urinary Tract*, DOI 10.1007/978-3-319-29219-9_12

Introduction

With advances in technology and technique, radiographic imaging of the urinary tract for pediatric patients has become progressively sophisticated for diagnosis and evaluation of urologic conditions. Due to its non-invasive nature and lack of radiation, ultrasonography is often utilized as the initial diagnostic tool for evaluation of the urinary tract. Importantly this modality is the primary imaging modality in the prenatal detection of genitourinary anomalies. Voiding cystourethrography and nuclear scintigraphy are also important diagnostic studies used in the postnatal patient that further aid in diagnosis and management. Over the last decade, computerized tomography (CT) and magnetic resonance imaging (MRI) have become more refined in providing clearer imaging with additional benefits to ultrasonography. These imaging modalities are fundamental in the management and treatment of patients with congenital urologic anomalies and will be discussed in detail in this chapter.

Imaging Modalities

Ultrasonography

Ultrasonography utilizes high-frequency sound waves to image organs and structures. It is one of the most important imaging modalities in the pediatric population. This relatively inexpensive study is frequently used since it is noninvasive and has the unique capability of visualizing structures in real time without exposure to radiation or nephrotoxic contrast agents. However, ultrasound provides no functional data, and the quality and clarity of the study is operator and equipment-dependent. Additionally impediments such as bowel gas and body habitus in older or obese children may limit visualization of structures and impact the quality of the exam [1].

Gray-scale, two-dimensional ultrasonography is the most commonly utilized mode for ultrasound. This pulsed-wave technique produces real-time images consisting of shades of gray as determined by the amplitudes of echoes reflected from the tissue. By convention, the liver is used as a benchmark to measure echogenicity of an image. Structures similar in brightness are considered isoechoic. Tissues with high-signal intensity, such as the peripelvic fat adjacent to the normal renal pelvis, appear brighter than the liver and are described as hyperechoic (Fig. 12.1). Hypoechoic tissues have less-intense signals relative to the liver and are transmitted as darker shades of gray, while those with no internal echo such as fluid or urine are anechoic and appear black on images (Fig. 12.2). Images are oriented with the cranial aspect of a structure to the left and the caudal aspect to the right. Three-dimensional and four-dimensional scanning are highly sophisticated modes of ultrasound utilized most commonly in obstetrics and prenatal imaging but have limited application in the routine evaluation of urinary anomalies postnatally due to its complex and expensive computational infrastructure.

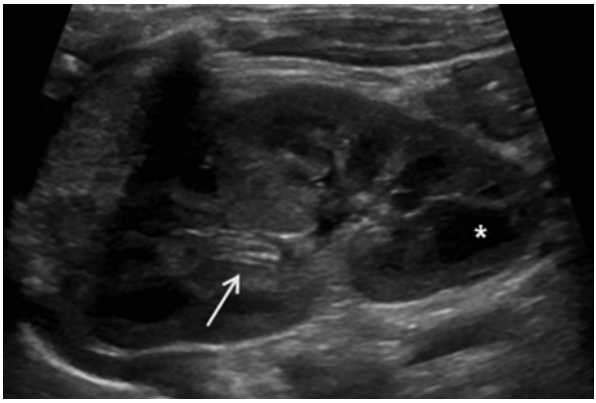

Fig. 12.1 Ultrasound of normal kidney. Hyperechoic peripelvic fat adjacent to the normal renal pelvis appears as white tissue in the central portion of the kidney as indicated by the *arrow*. Hypoechoic areas in the medulla of the kidney demonstrate normal corticomedullary differentiation and can be mistake for hydronephrosis (*asterisk*)

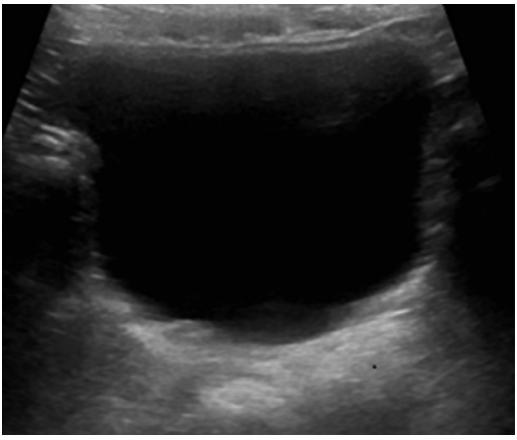

Fig. 12.2 Ultrasound of normal bladder. Urine within bladder appears black or anechoic

Doppler ultrasound mode is utilized for characterization of motion and is based on the principle of frequency shift when sound waves strike a moving target. Color Doppler is most commonly used to evaluate blood flow with the color blue indicating motion away from the transducer and the color red indicating motion toward the transducer. The velocity of motion is designated by the intensity of the color with higher speeds producing brighter hues.

Prenatal Ultrasonography

The number of routine prenatal ultrasounds performed in the United States has increased twofold between 1998 and 2005 [2]. Universally the sensitivity for detecting urologic anomalies before birth is high at 88 %. However, the overall sensitivity of the prenatal ultrasound varies for each disease process and is lower for congenital anomalies outside the genitourinary system [3].

By 16–17 weeks of gestation, the kidneys and bladder can be identified in 90 % of fetuses [4]. Bladder filling can be noted as early as 14–15 weeks which often

Fig. 12.3 Ultrasound of kidney from prenatal study. The kidney, surrounded by crosses, can be seen as hypoechoic paraspinal structure with a more echogenic renal pelvis. Pelviectasis is present as demonstrated by the central anechoic area (*arrow*)

allows identification of abnormalities such as ureteroceles, diverticula, or poor bladder emptying [5]. The kidneys appear as hypoechoic paraspinal structures with an echogenic renal pelvis (Fig. 12.3). Kidney length is measured to ensure appropriate growth for gestational age [6] (Table 12.1), and the kidneys are examined for evidence of hydronephrosis or abnormal cystic or solid structures. When hydronephrosis is noted, the degree and progression of dilatation often correlates with persistent postnatal pathology [7]. In one study 12 % of mild, 45 % of moderate and 88 % of severe hydronephrosis were associated with postnatal pathology [8]. The most commonly used method for defining antenatal hydronephrosis is anterior–posterior diameter (APD) of the renal pelvis. APD is determined by measuring the transverse axial image of the renal pelvis at the approximate level of the renal hilum. The Society for Fetal Urology (SFU) classification system is based on renal APD measurements in the second and third trimesters (Table 12.2) [9].

Amniotic fluid levels should be assessed especially in cases of bilateral hydronephrosis or when there is suspicion of poorly functioning kidneys. Oligohydramnios (defined as amniotic fluid index <5) and polyhydramnios (defined as amniotic fluid index >24) can indicate significant problems with urinary function and can be associated with complex congenital anomalies. Fetal urine chemistry compositions are an adjunct to prenatal imaging and allow classification of fetal renal function into good and poor functioning groups. While fetal management is beyond the scope of this chapter, prenatal imaging plays an important role in perinatal management and offers some insight into postnatal renal function (Refer to Chap. 13).

Abdominal Plain Film of Kidney, Ureter, Bladder (KUB)

While a plain abdominal film is the simplest radiographic study, its utility in congenital urologic anomalies is limited. A KUB is most useful in evaluating spinal or skeletal abnormalities which may indicate pathology such as spinal dysraphisms. It

Table 12.1 Normal fetal renal length during development

Renal length during development	
Gestational age	Length (cm)
18	2.2
19	2.3
20	2.6
21	2.7
22	2.7
23	3
24	3.1
25	3.3
26	3.4
27	3.5
28	3.4
29	3.6
30	3.8
31	3.7
32	4.1
33	4.0
34	4.2
35	4.2
36	4.2
37	4.2
38	4.4
39	4.2
40	4.3
41	4.5

With permission from Cohen HL, Cooper J, Eisenberg P, et al. Normal length of fetal kidneys: sonographic study in 397 obstetric patients. AJR Am J Roentgenol. 1991;157:545–8 [6]

Table 12.2 Classification scheme for grading hydronephrosis based on society for fetal urology consensus statement

Degree	Second trimester (mm)	Third trimester (mm)
Mild	4–<7	7–<9
Moderate	7–<10	9–<15
Severe	>10	>15

Data from Nguyen HT, Herndon CD, Cooper C, et al. The Society for Fetal Urology consensus statement on the evaluation and management of antenatal hydronephrosis. J Pediatr Urol. 2010;6:212–31 [9]

is also useful in the evaluation of bowel gas patterns and constipation. When combined with renal ultrasound, KUB can play an important role in the diagnosis of nephrolithiasis in the pediatric patient.

Intravenous pyelogram (IVP) is an antiquated study which is rarely used at the present time in pediatric urology. This contrast study begins with a scout KUB fol-

lowed by injection of an intravenous contrast. Images of the kidneys are then obtained during various stages of contrast uptake and drainage. IVP has ultimately been replaced by newer imaging techniques such as sonography and nuclear scintigraphy in the evaluation of hydronephrosis, and by CT scan in the evaluation of urolithiasis. One area where IVP may be useful is in acute trauma situations with an unstable patient and the need for evaluation of the renal collecting system. In this situation, 2 mL/kg of contrast is injected, and images are obtained approximately 10–20 min after contrast administration [10]. This may reveal renal pelvic or ureteral extravasation indicative of injury to the urinary tract and the need for surgical management.

Voiding Cystourethrography (VCUG)

The VCUG is a contrast imaging study which allows evaluation of the urinary bladder and urethra, and is the gold standard for the detection and grading of vesicoureteral reflux (VUR). A urethral catheter or feeding tube is placed in the bladder, and the bladder is filled to capacity with contrast medium. The study requires an initial scout KUB followed by fluoroscopic images of the bladder and upper urinary tract obtained during bladder filling and voiding.

During contrast instillation, filling detects are seen as darker areas surrounded by white contrast medium. The filling phase is important in identifying abnormalities such as ureteroceles since these structures may collapse and disappear as the bladder pressure increases with filling. Once the bladder is at full capacity, anteroposterior images and steep oblique images are obtained. This allows for identification of posterior bladder abnormalities including low grade reflux and bladder diverticula. Imaging during the voiding phase is important since 20 % of VUR may occur during the voiding phase and may be missed when these images are not included [11]. The voiding phase is also necessary for adequate visualization of the urethra. It is during this phase of the study that abnormalities such as a posterior urethral valve (PUV) and strictures are diagnosed. The voided volume is measured to determine actual bladder capacity in comparison to estimated bladder capacity (eBC): eBC (in ounces) = age (years) + 2 × 30) [10]. The efficiency of bladder emptying may also be determined.

When voiding is complete, the renal fossa should be examined as retained contrast from reflux may be visualized. With high grade reflux, a delayed abdominal film may be performed 15 min after voiding to differentiate simple reflux from reflux associated with ureteropelvic or ureterovesical junction obstruction [12]. Recent improvements to decrease radiation doses include low-dose fluoroscopy techniques and pulse fluoroscopy with digital enhancing modalities.

Nuclear Medicine Scintigraphy

Radionuclide Cystography (RNC)

Radionuclide cystography avoids the use of iodinated intravenous contrast agents, and is associated with lower radiation exposure as compared to contrast VCUG. Images are obtained from the patient's posterior position; therefore, right-sided structures are on the right side of the image and vice versa. It is ideal for patients requiring repeat imaging to evaluate resolution of VUR, for postoperative imaging after antireflux procedures, and/or sibling screening for reflux [10]. A dose of 0.5 mCi of Tc-99m-pertechnetate in isotonic saline is instilled into the bladder through a catheter. Continuous monitoring under a gamma camera provides a detailed cystogram and increases the sensitivity of the study without increasing ionizing radiation exposure to the patient. RNC offers limited detailed anatomic information of the bladder and urethra; however with continuous monitoring it is more sensitive than a VCUG for detection of VUR (Fig. 12.4) [10]. The determination of VUR grade is typically graded on a scale of 1–3 (Table 12.3) [13].

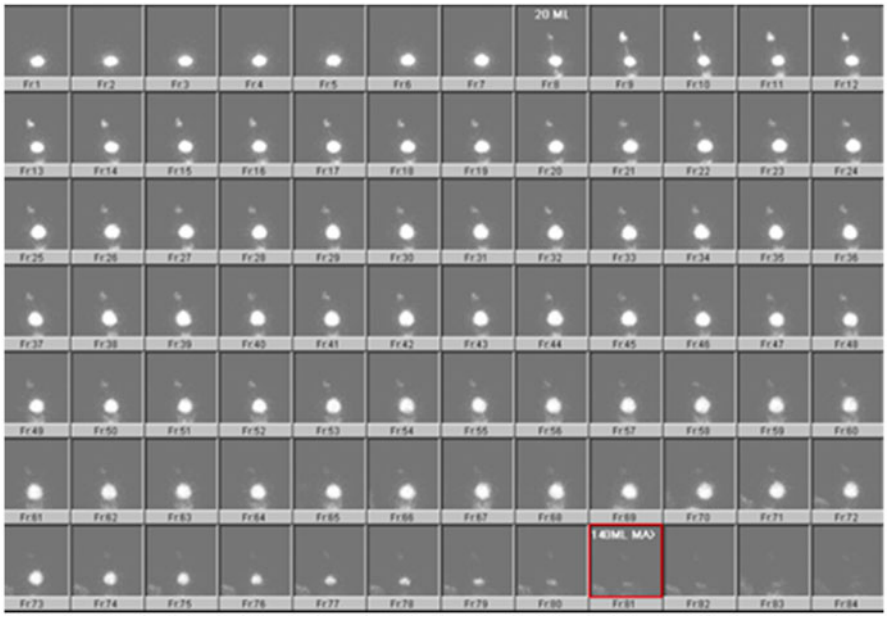

Fig. 12.4 Radionuclide cystogram. Mild left vesicoureteral reflux is first demonstrated at 20 mL of filling of the bladder and persists throughout filling and during voiding

Table 12.3 RNC grading system

RNC grade	International reflux grading system	Description
Grade 1	Grade 1	Activity limited to ureter
Grade 2	Grades 2–3	Activity reaching the collecting system with none or minimal activity in ureter
Grade 3	Grades 4–5	Dilatation of the collecting system and dilated tortuous ureter

Data from Willi U, Treves S. Radionuclide voiding cystography. Urol Radiol. 1983;5:161–73) [13]

Technetium-99m Dimercaptosuccinic Acid (DMSA)

Tc-99m-DMSA is a chelating agent taken up by and fixed to the proximal convoluted tubules in the renal cortex. There is little accumulation of the agent in the renal papilla and medulla with minimal excretion making it an excellent marker for renal cortical activity and function [12]. Renal scans are typically obtained 1.5–2 h after an intravenous injection of 0.05 mCi/kg of 99mTc-DMSA. Three techniques of imaging are performed: planar with parallel hole collimator, planar with parallel hole and pinhole collimator, and SPECT. Magnified posterior and posterior-oblique views are obtained using an ultrahigh resolution parallel collimator. DMSA scintigraphy is the gold standard for the diagnosis of acute pyelonephritis and is the best imaging modality to identify renal cortical scarring. It is also useful in the diagnosis of some congenital renal anomalies such as ectopic kidneys or ectopic ureters that may be associated with poorly functioning renal moieties or duplicated collecting systems. It provides accurate differential renal function of the kidneys and can even provide differential function between upper and lower pole moieties in a duplex system.

DMSA scan is the imaging modality of choice for diagnosing acute pyelonephritis which is demonstrated by decreased accumulation of the radiotracer inthe affected area (Fig. 12.5) [14]. Decreased uptake of radioisotope by tubular cells due to ischemia, inflammation, and/or decreased cellular enzyme function results in areas of diminished uptake of isotope on the final image defined as photopenia [4]. These areas of photon deficiency are associated with preservation of the normal renal contour. Over time these areas may resolve, and follow-up DMSA imaging may reveal normal appearing parenchyma with retained renal function or, alternatively, the insult may progress resulting in an irreversible renal scar characterized by parenchymal volume loss or a wedge defect associated with contraction of the damaged renal cortex (Fig. 12.6).

SPECT imaging using multidetector cameras has been applied to DMSA scans to increase sensitivity for detection of “defects” when compared to pinhole imaging. In an experimental study comparing pinhole and SPECT imaging to histology in a refluxing piglet model, SPECT was more sensitive (91 %) than pinhole imaging (86 %), however its specificity was lower (82 % compared with 95 %). The overall accuracy was 88.5 % for both [15].

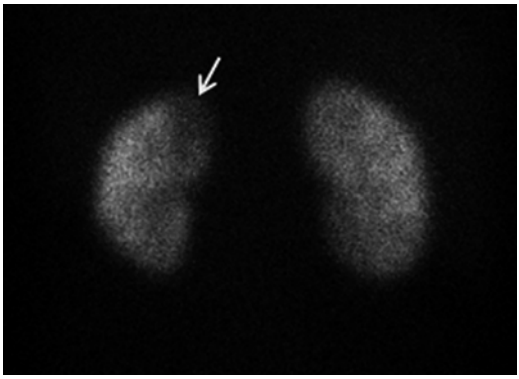

Fig. 12.5 DMSA scan showing acute pyelonephritis. Acute inflammation prevents normal radiotracer DMSA uptake and creates areas of photopenia as indicated by the *arrow*. However the normal renal contour is preserved

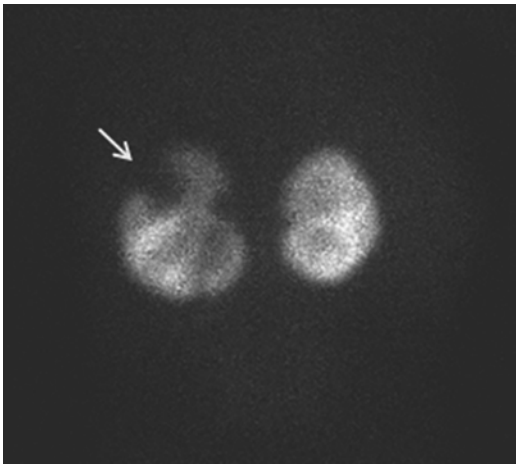

Fig. 12.6 DMSA scan showing renal scarring. Renal scarring results in photopenia associated with loss or contraction of the normal renal contour, as indicated by the *arrow*

Technetium 99m-Mercaptoacetyl Triglycine (MAG-3)

MAG-3 renal scan is the study of choice when both differential renal function and drainage of the renal collecting system require evaluation. Consequently, it is used primarily in the evaluation of hydronephrosis that may be secondary to an obstructive uropathy. MAG-3 is taken up by the proximal tubule and is cleared mainly by tubular secretion, independent of glomerular filtration rate. Patients are hydrated intravenously (15–20 mL/kg over 30–60 min), and a urinary catheter or feeding tube is inserted into the bladder and left in place to allow maximal bladder draining during the study. Images of the kidneys and bladder are obtained for 30 min after injection of 0.05 mCi/kg of radioisotope. A diuretic (furosemide 1 mg/kg; max 40 mg) is administered intravenously, and additional images are obtained for an additional 15–30 min to evaluate drainage of the collecting system. Various protocols exist for the timing of diuretic administration. Some institutions administer the diuretic 20 min prior to injection of the radioisotope, while others routinely inject at 15–30 min after administration of the radioisotope. Since filling and drainage of the collecting system can be affected by the severity of hydronephrosis, the patient's

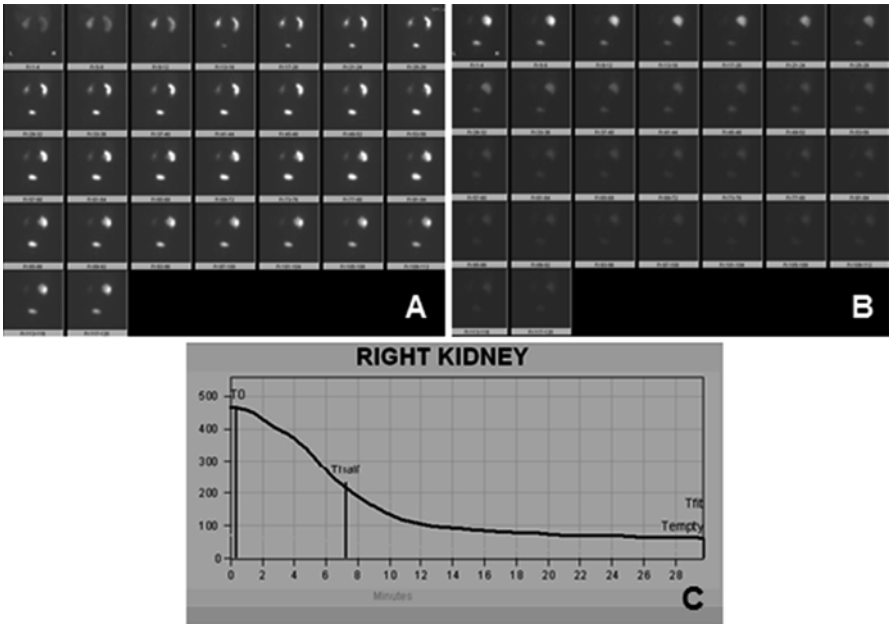

Fig. 12.7 MAG-3 scan demonstrating a non-obstructed kidney. Both kidneys demonstrate prompt uptake of radiotracer. (**a**) Pre-diuretic images reveal symmetric function determined in the first two images of uptake. There is prompt spontaneous drainage of radiotracer by the left system with retained radiotracer in the right system. (**b**) In post-diuretic images, the right kidney is cleared of radiotracer. (**c**) This is further depicted by the rapid downward slope of the drainage curve and a normal drainage T1/2 time of 7 min

hydration status, and the relative function of the involved kidney, we recommend that the collecting system should be maximally filled with radioisotope prior to administration of the diuretic. Additional images are obtained at 15–30 min after the administration of the diuretic to evaluate drainage of the collecting system. After 15 min of upright positioning, patients can be reimaged to assess for further clearance of the radioisotope resulting from gravity drainage.

Radiotracer counts are plotted on a time graph creating a three-phase curve [12]. The initial perfusion phase is characterized by a rapid rise in isotope counts reflecting blood flow to the kidneys. The renal phase follows and is used to assess differential renal function (DRF). In this phase, images are obtained 2–3 min following injection of the isotope before it gets excreted into the collecting system. In the final excretory phase, 1-min images are taken over a 30-min period and should demonstrate a gradual decline in radiotracer associated with drainage of urine from the kidney into the bladder. If retention of isotope is seen within a dilated renal pelvis or ureter, the diuretic is administered to increase urine flow in order to further assess drainage of the system. Drainage is determined by calculating the slope of the drainage curve in the excretory phase and the drainage half-time (T1/2). The T1/2 is defined as the time it takes for half of the isotope to clear from the collecting system. A non-obstructed kidney will demonstrate rapid washout of the radio-

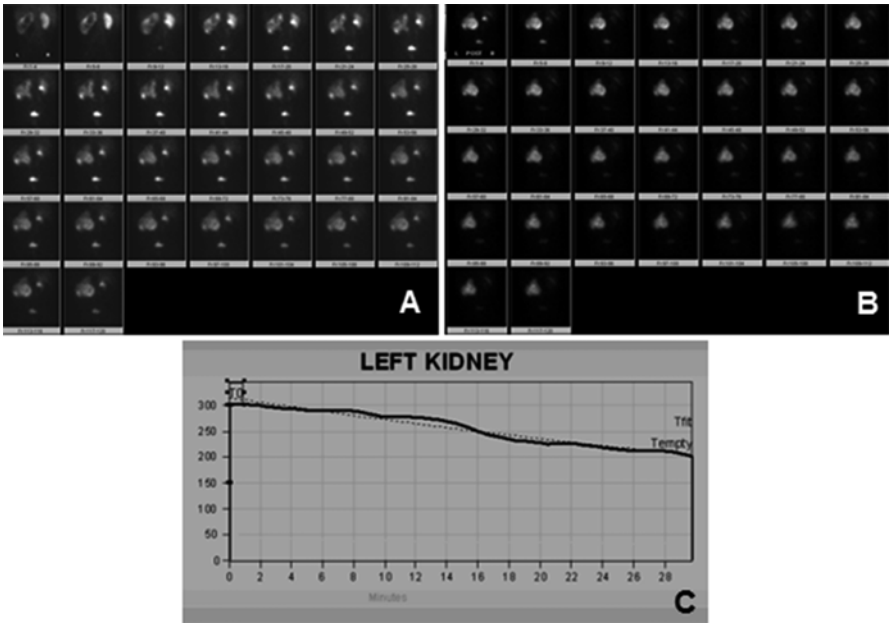

Fig. 12.8 MAG-3 scan demonstrating a ureteropelvic junction obstruction. (**a**) Pre-diuretic images reveal a central photopenic area in the left kidney due to the hydronephrosis in the first images. Prompt excretion of the radiotracer is seen by the right system with large volume retention of radiotracer in the left hydronephrotic system. (**b**) In the post-diuretic images, the dilated left kidney pelvis continues to retain the radiotracer. (**c**) This is further depicted by the very slow downward slope of the drainage curve compared to the steep downward slope in the non-obstructed system. The drainage T1/2 time is 51 min

tracer as indicated by a short T1/2 and a rapid downward slope of the drainage curve (Fig. 12.7). However, if the kidney is obstructed, the excretory phase will demonstrate a prolonged T1/2 associated with a slow and gradually declining or flattened curve, depending on the severity of the obstruction (Fig. 12.8). As obstruction becomes more severe, the relative renal function can become depressed and uptake of the radiotracer reduced. In cases of acute obstruction, prolonged cortical retention of radioisotope without filling of the collecting system may be visualized. Dehydration, poor renal function, and massive dilatation of the collecting system with urinary stasis may reduce the reliability of the diuretic renal scan.

The T1/2 has classically been used to determine drainage with <10 min considered normal drainage, 10–20 min considered indeterminate and >20 min considered obstructed. However, these values were determined in older children and adults. Recent studies have found that longer T1/2 in infants and young children may not indicate obstruction and may improve over time [16]. Since drainage half-times at one point in time have not been validated in infants, change in T1/2 over time is a more useful parameter to assess for progressive or persistent obstruction. The exception is when there is a flat or rising drainage curve and/or when delayed drainage is associated with ipsilateral reduced DRF below 35–40%, indicating high-grade obstruction.

Computed Tomography (CT)

CT scans have become an integral part of urologic practice for general conditions. However, its use for congenital genitourinary disorders is quite limited due to the relatively high amount of radiation exposure to an infant and possible nephrotoxicity of iodinated contrast. The basis of CT imaging is the attenuation of x-ray photons as they pass through different body tissues. A computer then reconstructs cross-sectional images of the body based on measurements of X-ray transmission through thin slices of the body tissue [17]. In general, three phases of a CT scan can be obtained in urologic practice. The initial, non-contrast CT phase is utilized to evaluate hydronephrosis, stones, renal parenchymal calcifications, or renal cysts. With the administration of intravenous contrast, an arterial and nephrogenic phase can be obtained to allow evaluation of vascular anatomy and abnormalities such as renal masses which notably enhance with the contrast. Finally delayed phase images, taken when the contrast enters and fills the renal collecting system, are used to detect filling defects, hydronephrosis, or extravasation of contrast from the collecting system. In spite of CT imaging advantages, it is rarely in infants used given the alternative imaging modalities of ultrasonography, nuclear medicine scans, and MRI scans which provide sufficient information with significantly less radiation to the developing child.

Magnetic Resonance Imaging

Improvements in technology and growing availability have led to an increase in the use of MRI in the evaluation of the genitourinary system. MRI acquires images based on proton density, T1 and T2 relaxation flow, magnetic susceptibility, and diffusion [4]. To obtain an MRI sequence, radiofrequency pulses are transmitted through the patient via a radiofrequency antenna or "coil." When the pulse stops, protons release their energy, and they are detected and processed to obtain the image. Weighting of the image is dependent on the energy imparted through the physics of the pulse sequence, and whether the energy is released slowly or quickly; images are described as being T1- or T2-weighted. On T1-weighted images, fluid has a low signal and appears dark, while on T2-weighted images signals are high and appear bright. Intravenous gadolinium contrast is administered to augment the relaxation of protons on T1-weighted images, making the kidney brighter and increasing the possibility of the detection and characterization of renal masses [1].

Currently MRI is reserved for evaluation of more complex pediatric urological anomalies. MRI can provide excellent details of the genitourinary system in the fetus or in neonates and children without radiation exposure [18]. It can delineate fine details to determine anatomic relationships making it a valuable imaging modality in the evaluation of congenital abdominal and pelvic masses, and duplicated collecting systems with ectopic ureters. Advances in MRI technology have allowed functional assessment of the renal system, including differential renal function and drainage of hydronephrotic kidneys. It has also been reported to be superior to renal scintigraphy for the diagnosis of pyelonephritis and renal scarring. However,

direct comparison with histology in a refluxing infected piglet model showed similar accuracy between these imaging modalities [19, 20]. Limitations include its relative high expense and limited availability in comparison to other imaging modalities. Additionally, most children require heavy sedation or anesthesia.

Congenital Anomalies

Kidney/Adrenal

Congenital Hydronephrosis

Antenatal hydronephrosis is the most common urologic abnormality identified on prenatal ultrasonography [1]. Numerous grading systems have been developed in an attempt to adequately describe antenatal hydronephrosis. However, there is no consensus on the best method of reporting the degree of dilatation [1]. The most common method is the anterior–posterior diameter (APD) (Table 12.2). While this provides adequate information for pelvic dilatation, it does not adequately describe pelvic configuration or calyceal dilatation, and it offers little information on the appearance of the renal parenchyma. The 4-scale SFU grading system is the most commonly used system for postnatal ultrasound (Fig. 12.9) [21].

The differential diagnosis for antenatal hydronephrosis is expansive (Table 12.4). However the vast majority of cases (64%) are due to non-obstructed, transient hydronephrosis which resolves spontaneously over time [7]. Patients diagnosed with hydronephrosis may require extensive prenatal imaging with serial ultrasounds or MRI. Postnatal studies are often required and include ultrasound, VCUG, and/or functional or diuretic renograms. The need for further testing is determined by the grade of hydronephrosis seen on postnatal ultrasound and any additional abnormalities such as hydroureter. Postnatal evaluation with diuretic renography or MRI is usually reserved for patients with persistent SFU grade 3 and grade 4 hydronephrosis. If a postnatal sonogram is performed within the first several days of life, a repeat exam is necessary to avoid underestimating the severity of hydronephrosis that can be caused by perinatal dehydration.

Ureteropelvic Junction (UPJ) Obstruction

The most common pathologic etiology of antenatal hydronephrosis is UPJ obstruction. Kidneys with UPJ obstruction may have varying degrees of renal pelvis dilation, variation in calyceal dilation and thinning of the renal parenchyma. In severe cases, cystic changes may also be seen indicating dysplasia. Congenital UPJ obstruction may present later in childhood or adolescence with flank or abdominal pain which is often cyclic and associated with nausea and vomiting. These symptoms are referred to as a Dietl's crisis and should prompt initial evaluation with renal ultrasonography. Other presentations in older children include urinary tract

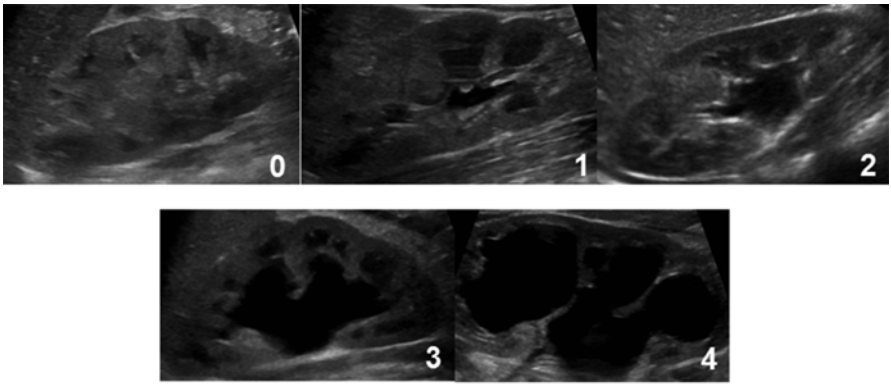

Grade of Hydronephrosis	Renal Pelvis	Renal Parenchymal Thickness
Grade 0	No dilatation	Normal
Grade 1	Mild dilatation; splitting of renal pelvis	Normal
Grade 2	Moderate dilatation but limited to renal pelvis	Normal
Grade 3	Marked dilatation, renal pelvis and calyces are dilated	Normal
Grade 4	Severe dilatation of renal pelvis and calyces	Thinned

Fig. 12.9 SFU grading system for hydronephrosis. With permission from Fernbach SK, Maizels M, Conway JJ. Ultrasound grading of hydronephrosis: introduction to the system used by the Society of Fetal Urology. Pediatr Radiol. 1993;23:478. (11)

Table 12.4 Differential diagnosis for antenatal hydronephrosis, categorized based on level of dilatation

Renal pelvis	Renal pelvis and ureter	Renal pelvis, ureter, bladder, and possibly urethra
UPJ obstruction	VUR	PUV
VUR	UVJ obstruction	Neuropathic bladder
MCDK	Nonobstructed megaureter	Urethral aplasia
ADPKD	Ectopic ureter	
	Ureterocele	
	Prune-belly syndrome	

infection or hematuria, especially following minor trauma, and less commonly, kidney stone formation.

If a UPJ obstruction is suspected on ultrasonography, a MAG-3 diuretic renal scan is the imaging modality of choice to confirm the diagnosis. This study provides a quantitative assessment of DRF as well as the drainage of the dilated collecting

system. When MAG-3 imaging reveals a poorly draining system, two options are available: expectant surveillance or operative intervention. Surveillance is typically recommended for asymptomatic infants who have indeterminate drainage curves associated with preserved renal function of greater than 35–40 %. An indeterminate curve often slopes downward slowly, the T1/2 is greater than 20 min, and the collecting system may reveal incomplete emptying of the collecting system with retained radioisotope, even with gravity drainage. Spontaneous resolution or improvement of hydronephrosis has been reported in up to 78 % of kidneys with moderate or severe hydronephrosis and a differential function of greater than 35 %. However, careful follow-up is warranted because more than 30 % of UPJ obstruction cases may require pyeloplasty [22]. Follow-up includes serial sonograms with periodic MAG-3 diuretic renal scans at 6- to 12-month intervals, depending on the degree of obstruction and progression of hydronephrosis.

Indications for surgical intervention in the neonate with antenatal hydronephrosis include poor initial DRF (<35–40 %) or subsequent deterioration of DRF during follow-up, lack of significant drainage despite furosemide administration (flat or rising drainage curve), worsening drainage over time, and persistent obstruction with stable DRF but no evidence of improvement after 4–5 years of observation [10]. In contrast to asymptomatic infants, older children with UPJ obstruction who present with symptoms such as abdominal/flank pain, infection, or hematuria are usually managed by operative intervention.

Renal Cystic Disease

Multicystic dysplastic kidney (MCDK) is characterized sonographically by multiple noncommunicating cysts, minimal or absent parenchyma, and the absence of a central large cyst. By definition multicystic kidneys do not function. It is important to differentiate between a non-functioning MCDK and severe hydronephrosis with dysplasia where the renal pelvis and calyces communicate, and renal scintigraphy will reveal varying degrees of reduced renal function (Fig. 12.10) [1]. The natural history of MCDK is benign, and typically the kidney will spontaneously involute over time. Although the contralateral kidney usually demonstrates compensatory hypertrophy, in some cases the contralateral kidney may also be abnormal. Contralateral UPJ obstruction has been reported in 3–12 %, while VUR has been reported in as many as 18–43 % [1]. Radiographic evaluation of a MCDK can include a DMSA or MAG-3 scan to confirm the absence of function if the diagnosis of MCDK cannot be clearly established by sonography. A VCUG may also be considered to evaluate for contralateral reflux. However, some authors advocate that VCUG has little value in the absence of infection if sonography is consistent with a MCDK and the contralateral kidney appears normal [23]. Nonsurgical surveillance with a follow-up ultrasound in 6–12 months to monitor for involution is routinely recommended. Nephrectomy is rarely indicated due to the high rate of spontaneous involution and the absence of symptomatology associated with MCKD. Since hypertension has occasionally been noted in these children, yearly blood pressure monitoring is recommended.

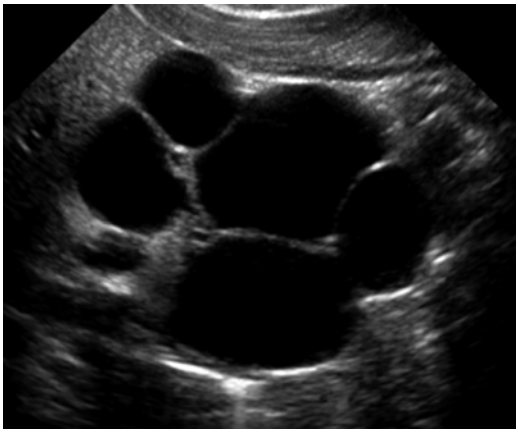

Fig. 12.10 Ultrasound of multicystic dysplastic kidney. Classic findings of multiple non-communicating cysts and absent parenchyma are seen

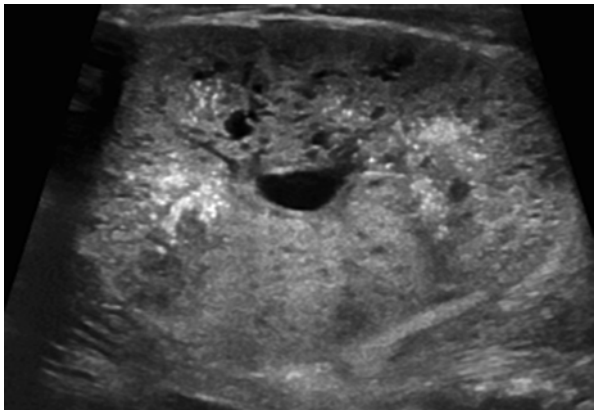

Fig. 12.11 Ultrasound of autosomal recessive polycystic kidney. Kidneys are typically massively enlarged and diffusely echogenic or bright. This kidney in a newborn measures 7 cm (normal size 4–6 cm)

Autosomal recessive polycystic kidney disease (ARPKD) affects 1 in 10,000–50,000 live births. However as many as 50 % of affected newborns die in the first few days of life [1]. ARPKD may be detected prenatally with ultrasound imaging revealing symmetrically enlarged hyperechoic kidneys, enlarging fetal abdominal circumference, and oligohydramnios (Fig. 12.11). Postnatally imaging is required for evaluation of other organs such as the spleen and liver due to the presence of congenital hepatic fibrosis

Autosomal dominant polycystic kidney disease (ADPKD) is the most common inheritable form of renal cystic disease and affects 1 in 400–1000 live births [1]. While it is most commonly identified in adulthood, it has been reported in 2–5 % of newborns and infants [24]. When ADPKD is manifested in the fetus or neonate, 50 % of affected kidneys are large with identifiable macrocysts on ultrasound. Over time, cysts usually enlarge and increase in number [1]. Cysts are often noted in the liver, pancreas, spleen, and lungs; aneurysms of the circle of Willis, aortic aneurysms and mitral valve prolapse are common associated anomalies. Renal failure has been reported in 7–15 % of patients with ADPKD, most commonly in the adult population.

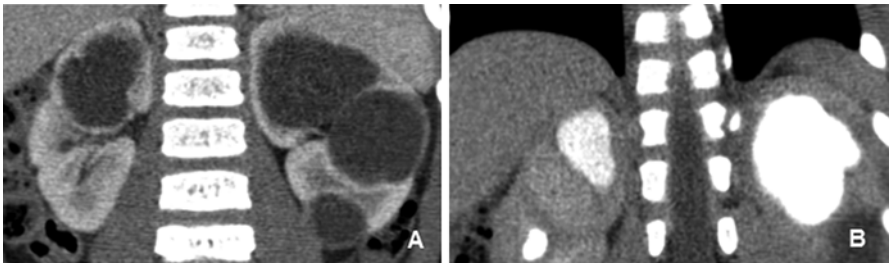

Fig. 12.12 CT scan of calyceal diverticulum with delayed images. (**a**) During the nephrogenic phase, the fluid filled structures within the kidneys appear as large simple cysts. (**b**) During the delayed phase, contrast is seen filtering into these fluid-filled structures, indicating calyceal diverticula

Simple cysts are rare but may occur in infants and present as round or ovoid, anechoic structures with sharply defined, smooth walls on ultrasound. Given the benign nature, long-term follow-up is not required. However, a repeat sonogram after 1 year of age is recommended to monitor for significant increases in size or changes in characteristics of the cyst. A calyceal diverticulum is often confused with a simple cyst. The calyceal diverticulum is an outpouching of the collecting system into the corticomedullary region of the kidney. It is connected to the renal pelvis via a narrow infundibulum. Calyceal diverticula are usually asymptomatic but may cause flank pain or result in stone formation due to stasis of urine. To differentiate between a simple cyst and a calyceal diverticulum, a MAG-3 renal scan or contrast CT with delayed images should be obtained. Delayed filling of the calyceal diverticulum or retention of radioisotope or contrast on imaging is diagnostic (Fig. 12.12).

Tumors

Solid masses in a newborn are rare but may be detected on prenatal ultrasound. Due to suboptimal visualization of masses on ultrasonography, contrast CT or MRI is often utilized to better characterize the mass and determine tumor consistency, extent of local disease, and distant organ involvement. Subtle differences may give some indication of the diagnosis. However, confirmatory histologic evaluation is necessary.

Although congenital mesoblastic nephroma is rare, it is the most common solid renal tumor in the neonatal period and the most common renal tumor diagnosed on prenatal imaging. Prenatal diagnosis via ultrasound has been made as early as 22 weeks of gestation and is suggested when a vascular ring sign or an anechoic ring surrounding the tumor is noted [25, 26]. Nephrectomy is considered curative in classic mesoblastic nephroma, although the cellular variant can recur locally or metastasize. Diagnosis in the newborn period is most often associated with the classic variant, while children diagnosed after 3 months of age may manifest the more aggressive cellular variant. Chaudry et al utilized CT, MRI and ultrasound imaging in 30 children (15 boys, 15 girls) with congenital mesoblastic nephroma to determine if imaging could characteristics could determine the classic versus cellular variant. They noted that findings suggestive of the classic variant included a periph-

eral hypoechoic ring or a large solid component, whereas cystic/necrotic changes and hemorrhage were more common in the cellular variant. They also noted that cystic components were readily identified on ultrasonography, central hemorrhage was easily identified on CT scanning, and MRI was highly sensitive for cystic components and central hemorrhage [27].

Congenital rhabdoid tumor of the kidney and Wilms tumor or renal nephroblastoma, are extremely rare congenital malignancies, but are quite aggressive when they occur. Rhabdoid tumor of the kidney is the most aggressive and lethal childhood renal tumor with a propensity to metastasize to the brain; therefore brain imaging with CT or MRI is vital. Case reports of Wilms tumor have been reported prenatally but typically present later in childhood. Initial screening is usually performed via ultrasound; however, if a suspicious lesion is present, contrast-enhanced CT or MRI should be performed.

The differential diagnosis of prenatally diagnosed adrenal masses includes neuroblastoma, adrenal hemorrhage, adrenal cysts, adrenal adenoma and carcinoma. Neuroblastoma is the most common extracranial solid tumor of childhood, and over half of children present with metastatic disease. Imaging studies play an important role in the evaluation of a child with neuroblastoma. Plain radiographs may demonstrate a calcified abdominal or posterior mediastinal mass. Contrast enhanced CT and MRI provide detailed information on the extent of disease. The finding of calcifications within the tumor and vascular encasement, or both, on CT is highly suggestive of neuroblastoma and helps differentiate it from Wilms tumor [28]. Currently the Children's Oncology Group protocols require both a radionuclide bone scan and meta-iodobenzylguanidine (MIBG) scan for staging [29]. While adrenal adenomas and carcinomas are extremely rare in the neonatal period, adrenal hemorrhage is relatively common and may occur in 1–2 % of healthy infants. Predisposing factors include prolonged labor, birth trauma, and large birth weight [1]. Ultrasonography reveals an echogenic suprarenal mass, with a late appearance of peripheral eggshell calcifications in contrast to stippled calcifications of neuroblastoma. Management of adrenal hemorrhage is always supportive and expectant.

Renal Anomalies

In utero, multiple anomalies can occur to the kidney ranging from complete absence to aberrant location, orientation, and shape of the kidney. These findings are often detected on prenatal ultrasound imaging or incidentally later in life. While bilateral renal agenesis is lethal, unilateral renal agenesis occurs in 1 in 1100 births, more frequently on the left side. The ipsilateral ureter is completely absent in about 60 % of cases [1]. It has been postulated that renal agenesis may be due to an involuted MCDK. The postnatal diagnosis is established by ultrasound which reveals a solitary kidney with compensatory hypertrophy. If renal agenesis is suspected, it is reasonable to confirm with a MAG-3 or DMSA renal scan to ensure a small ectopic kidney has not been missed.

Renal ectopia occurs when the kidney is outside of the normal anatomical location. Variants include anomalies of renal ascent where the kidney can be found in

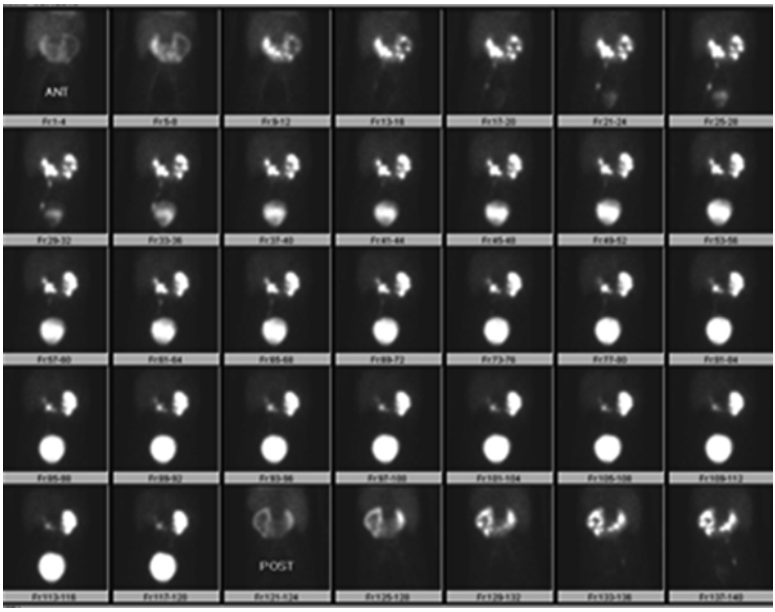

Fig. 12.13 MAG-3 scan demonstrating a horseshoe kidney. Due to the anterior location of horseshoe kidneys, a radiologist may invert the image anterior to posterior for better visualization of the kidneys as seen in the first four rows of this image. This pre-diuretic image demonstrates good drainage of the right system with retention of isotope within the dilated left system

the pelvis, lumbar region, or rarely the thoracic cage. In some cases, renal ectopia is associated with anomalies of renal fusion or form. The horseshoe kidney is the most common of all renal fusion anomalies and occurs in 1 in 400 births. It is possibly associated with an increased incidence of UPJ obstruction, and therefore a MAG-3 renal scan may be warranted to assess for urinary drainage if moderate or severe hydronephrosis is present (Fig. 12.13). In cases of crossed fused renal ectopia, the kidney crosses the midline to fuse with the contralateral kidney. These anomalies are often associated with aberrant vascular supply with an unpredictable pattern. This is important to note if surgical intervention is required. While ultrasonography detects these anomalies initially, DMSA or MAG-3 renal scan may provide further anatomical and functional confirmation.

Ureter

Vesicoureteral Reflux (VUR)

VUR is a common postnatal diagnosis for patients with antenatal hydronephrosis, although the severity of hydronephrosis itself may not be indicative of the presence of VUR and may not prompt the appropriate postnatal workup [7]. Authors have suggested that other parameters including hydroureter, renal duplication anomalies, and renal dysmorphia on initial sonography may be more useful for subsequent

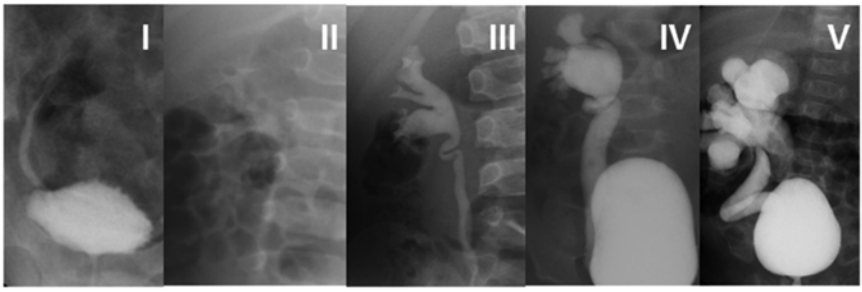

Grade of VUR	Description
Grade I	VUR does not reach the renal pelvis.
Grade II	VUR extends up to the renal pelvis without dilation.
Grade III	Mild or moderate dilation of the ureter and the renal pelvis. No or slight blunting of the fornices.
Grade IV	Moderate dilation of the ureter, renal pelvis, and calyces. Complete obliteration of the sharp angle of the fornices but maintenance of the papillary impression in most calyces.
Grade V	Gross dilation and tortuosity of the ureter. Gross dilation of the renal pelvis and calyces. The papillary impressions are not visible in most calyces.

Fig. 12.14 The international reflux grading system for VCUG. With permission from Fernbach SK, Feinstein KA, Schmidt MB. Pediatric voiding cystourethrography: a pictorial guide. Radiographics. 2000;20:155–71. (11)

detection of reflux [30]. Reflux is graded according to the International Reflux Study in Children (Fig. 12.14) [11]. While reflux alone does not harm the kidney, in the presence of infection and VUR significantly increases the risk of pyelonephritis and renal scarring. Since most VUR detected prenatally is high grade, newborns should remain on antibiotic prophylaxis to prevent infection until VUR is evaluated with VCUG. For higher grades of reflux, a DMSA scan is oftentimes obtained to assess for congenital reflux nephropathy and to determine differential renal function. Abnormalities on DMSA scan may be diffuse or segmental areas of decreased uptake of radioisotope resulting from congenital hypoplasia or dysplasia. These congenital defects may appear similar in some cases to those that are caused by post-pyelonephritic renal scarring. Differentiation between renal scarring and

congenital reflux nephropathy is based on the presence or absence of a history of culture-documented urinary tract infection (UTI).

In contrast to infants diagnosed after UTI, prenatally diagnosed VUR occurs more frequently in males and is often high grade reflux [31]. Interestingly, prenatally detected VUR is associated with higher rates of spontaneous resolution or improvement compared with similar grades of VUR diagnosed following urinary infection, particularly in older infants and children. Spontaneous resolution of VUR over time has been reported in up to 43 % in patients with high grade reflux detected prenatally [32]. Follow-up recommendations include a VCUG or RNC at 18- to 24-month intervals and continuous antibiotic prophylaxis until resolution of the reflux or until sufficient improvement in a child who is toilet trained [33].

Megaureter

Megaureter is a generic term indicating the presence of an enlarged ureter measuring greater than 7 mm in diameter with or without concomitant dilatation of the renal collecting system. Megaureter is characterized as congenital primary megaureter or secondary megaureter when associated with anatomical or functional bladder outlet obstruction. Megaureter can be classified further as obstructed or non-obstructed, refluxing or non-refluxing, and, in rare cases, both refluxing and obstructed [34]. Initially the abnormal finding of a dilated ureter is found on ultrasonography. To further delineate the pathology, a VCUG is obtained to look for VUR and evaluate the bladder and urethra for other causes of ureteral dilation including ureterocele, ectopic ureter, PUV in boys, or neuropathic bladder. A MAG-3 renal scan is often necessary to evaluate the differential renal function and to determine drainage of the dilated ureter. The natural history of a non-refluxing, non-obstructed primary megaureter is spontaneous improvement or resolution in over 70 % [35, 36]. Serial ultrasonography is a safe and appropriate method for following these patients when there is preserved renal function of the involved kidney on MAG-3 renal scan and an established pattern of improving hydroureteronephrosis. Corrective surgery may become necessary if MAG-3 diuretic renal scintigraphy indicates high grade obstruction or if hydronephrosis worsens during follow-up. If the megaureter is associated with VUR and it does not improve or is associated with breakthrough UTIs, surgery may be indicated.

More extreme forms of megaureter are seen with anomalies such as megacystis-megaureter and prune-belly syndrome. Megacystis-megaureter occurs when massive bilateral reflux causes a gradual remodeling of the entire urinary tract as the urine yo-yo's between the bladder and ureters. This phenomenon can be identified initially via ultrasound as a massively dilated, thin-walled bladder and dilated upper tract. Diagnosis is confirmed with VCUG which reveals a large smooth-walled bladder associated with severe high grade VUR. Megacystis-megaureter can be confused with prune-belly syndrome where similar findings can be seen on VCUG. However, prune-belly syndrome presents with a constellation of other findings including lack of abdominal wall musculature, bilateral cryptorchidism, dilated

posterior urethra due to prostatic hypoplasia, and other non-urologic abnormalities. In addition to severe bilateral hydroureteronephrosis which may be seen on ultrasound, patients with prune-belly syndrome may demonstrate increased renal parenchymal echogenicity, cystic changes, and poor corticomedullary differentiation indicative of renal dysplasia. Due to the risk of progressive renal insufficiency, these patients require long-term monitoring of the hydronephrosis as well as bladder and kidney function.

Ureteral Anomalies

Other ureteral anomalies can be identified with prenatal ultrasonography. Ureteral duplication is relatively common and may be characterized as simple or complex. A simple duplication is demonstrated by a larger-than-normal kidney associated with the sonographic finding of two central hyperechoic foci representing the renal perihilar fat separated by a band of normal echogenic renal parenchyma. There is no evidence of associated hydronephrosis or hydroureter, and the bladder is normal [34]. No additional imaging studies are indicated for these normal variants as they are not associated with an increased risk of infection.

Complex renal duplication occurs in approximately 4.7 % of patients with ureteral anomalies and is associated with dilatation of the fetal urinary tract [37]. More complex cases are associated with ureteroceles, ectopic ureters, UPJ obstruction, or VUR. Ultrasound may reveal variable degrees of hydronephrosis of the upper and/or lower pole moiety. Hydroureteronephrosis of the upper pole moiety is more often associated with an ectopic ureter or ureterocele. Ureterocele is a cystic dilation of the distal aspect of the terminal ureter and is seen on ultrasound as a thin-walled, balloon-like structure protruding into the bladder. Ureteroceles are most often associated with ureteral duplications (80 %) but can occur in single systems [1].

In the absence of a ureterocele, upper pole hydroureteronephrosis suggests an ectopic ureter [38]. Ectopic ureters may terminate in the bladder neck or proximal urethra in boys and girls, in the seminal vesicles or vas deferens in boys, or in the distal urethra or vagina in girls. Termination in girls below the external urethral sphincter will result in constant urinary incontinence most often noted after the child is toilet-trained. In boys, insertion of the ureter proximal to the external sphincter prevents continuous leakage. However, if the insertion site is in the vas deferens or seminal vesicles, UTI may be the presenting symptom. Dilation of the lower pole moiety is most often associated with high grade VUR and less commonly with lower pole UPJ obstruction [34]. VUR associated with a duplex system usually is only seen into the lower moiety unless the duplication is incomplete and both ureters empty into a short common stem near the bladder or in a submucosal segment of the ureter. The risk of urinary infection is significantly increased in these anomalies.

Following initial ultrasound, a VCUG should be obtained to evaluate the presence of reflux and to evaluate the bladder for abnormalities such as ureteroceles. VUR into the lower moiety of a duplex system typically is associated with a “drooping lily” appearance of the lower pole collecting system caused by lateral and downward dis-

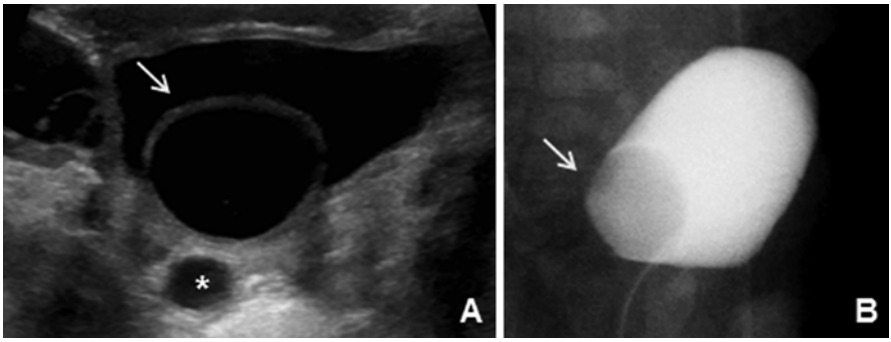

Fig. 12.15 Ultrasound and VCUG demonstrating a ureterocele. (**a**) The ultrasound demonstrates a thin-wall cystic structure within the bladder (*arrow*) with an associated dilated ureter (*asterisk*). (**b**) VCUG demonstrates a filling defect near the trigone, early in filling (*arrow*)

placement by the non-visualized upper moiety. The collecting system opacified by contrast usually demonstrates only two major infundibula and an incomplete set of calyces which are more laterally positioned and associated with a more vertical axis. Ureteroceles are typically detected during the early filling phase of the bladder as a smooth, round filling defect (Fig. 12.15). It is prudent to evaluate the voiding phase of the VCUG as reflux into an upper pole ectopic ureter may only occur while the bladder neck is open during voiding. In complex duplicated collecting systems, a MAG-3 renal scan can provide both functional and drainage information for each system. Typically the upper pole moiety associated with an ectopic ureter or ureterocele will reveal severely diminished function and delayed drainage. However, some upper pole moieties with non-obstructing ureteroceles or ectopic ureters in the bladder will have better preservation of function and non-obstructed drainage on a furosemide MAG-3 renal scan. A DMSA scan may be useful to assess renal function in cases where reflux is present in the duplex system. Magnetic resonance urography is less commonly used but may be helpful in defining complex anatomic relationships.

Bladder

Diverticula

Bladder diverticula are found in approximately 1.7 % of children [39]. A paraureteral diverticulum can develop dorsal or lateral to the ureteral orifice and is often associated with VUR. Stasis within a large, poorly draining diverticulum with a narrow neck is often associated with an increased risk of UTI. While ultrasonography may detect these lesions, they are best viewed on a VCUG with oblique views. This provides anatomical detail and can assess emptying of the diverticulum after voiding. While bladder masses occur rarely in children, they are almost never congenital and therefore are not discussed.

Urachal Anomalies

Anomalies of the urachus, the embryonic remnant of the communication between the bladder and umbilicus, include urachal sinus, urachal cyst, patent urachus, and urachal diverticulum. Patients most often present after birth with periumbilical discharge. In these cases the differential diagnosis includes an umbilical granuloma or patent omphalomesenteric duct. Older patients are more likely to present with a periumbilical mass or cyst and abdominal or periumbilical pain. Ultrasonography is the initial diagnostic imaging modality of choice and may reveal a cystic appearing mass at the most superior aspect of the bladder. VCUG is often necessary to determine if there is communication between the bladder and the urachal remnant or if there is a blind-ending sinus. Alternatively, a sinogram can be performed by instilling contrast into the umbilical opening. CT or MRI may also be used if the ultrasound or VCUG is non-diagnostic.

Exstrophy

The exstrophic complex of anomalies of the bladder ranges from the mildest form of epispadias to cloacal exstrophy. The most common anomaly is classic bladder exstrophy. Prenatal ultrasound may suggest bladder exstrophy in a fetus by absence of bladder filling or non-visualization of the bladder, a low-set umbilicus, widening of the pubic rami, and diminutive genitalia [1]. Cloacal exstrophy is the most severe manifestation of the exstrophy–epispadias complex, carrying all the findings associated with bladder exstrophy and renal, spinal, and bowel involvement in the form of a lateral enterovesical fistula. Complex cysts in the pelvis noted on prenatal ultrasound raise suspicion for cloacal exstrophy. However, like the classic variant, cloacal exstrophy is possible when the bladder is not visualized. Because of prolapsed ileum, cloacal exstrophy may be confused on prenatal sonography with omphalocele. Although sonography is an excellent modality to evaluate the fetus, factors such as maternal body habitus and/or oligohydramnios can prevent an adequate assessment of fetal anatomy, and ultrasound may not be adequate. Prenatal MRI has become an important imaging study in these cases. Children born with any exstrophic complex abnormality will require complex treatment and full evaluation of the skeletal, genitourinary, and reproductive systems.

Neuropathic Bladder

The most common cause of a neuropathic bladder in infants is due to spina bifida. This may initially be detected on prenatal screening with α-fetoprotein and ultrasonography where a small posterior fossa, small cerebellum, effaced cisterna magna, or ventriculomegaly may be visualized. Diagnosis may be made postnatally based on physical examination of the lower back as well as on plain film as an abnormality of the spine or sacrum or on spinal ultrasound or MRI. Along with the other neurologic

implications of the entity, a neuropathic bladder and bowel commonly develop which manifest as significant bladder and bowel dysfunction. Infants with spina bifida should be evaluated by renal/bladder ultrasound to evaluate the upper tracts for hydronephrosis or hydroureteronephrosis that may be secondary to a high pressure bladder associated with functional bladder outlet obstruction from an overactive or dyssynergic external sphincter. In these cases, the bladder may be thick-walled or trabeculated. The ultrasound should be repeated yearly to monitor the urinary tract for progressive changes. A VCUG is also warranted to diagnose secondary VUR which occurs due to elevated bladder pressures. It may confirm bladder wall trabeculations with diverticula that may not be appreciated on ultrasound [33].

Urethra

Posterior Urethral Valve

Posterior urethral valve (PUV) can result in prenatally detected hydronephrosis in male fetuses. Prenatal ultrasound findings may include a distended bladder with a thickened bladder wall and unilateral or bilateral hydronephrosis or hydroureter. Prenatal sonography of the bladder may show a "keyhole" sign, representing the dilated prostatic urethra immediately below the distended bladder. In severe cases, kidneys may be severely hydronephrotic with increased echogenicity or cystic changes in renal parenchyma suggestive of dysplasia. Oligohydramnios may be noted. Postnatal outcomes are worse when these findings are detected before 24 weeks of gestation.

Postnatally, a 5–6 French feeding tube or urethral catheter without a balloon should be placed, and urine output and renal function should be monitored closely. A definitive diagnosis is made with a VCUG which demonstrates a dilated posterior urethra and an abrupt transition point with a narrow caliber distal urethra at the location of the valve (Fig. 12.16). The bladder neck is often prominent due to hypertrophy and may appear as an annular band. The valve bladder can be irregular with trabeculations, diverticula, and bladder wall thickening. VUR is present in 50 % of cases and is often severe [40].

The function of each renal unit can vary and may be equal or asymmetrical. In some cases unilateral high-grade reflux is present and secondary to the high bladder pressure. The "pop-off" mechanism to relieve the high intravesical pressure allows the contralateral kidney to develop normally but often sacrifices the function of the refluxing kidney. This phenomenon is called VURD syndrome (posterior urethral valve, unilateral vesicoureteral reflux, and renal dysplasia). Bladder diverticula, a patent urachus, and urinoma may also act as "pop-off" mechanisms, preserving renal function by lowering bladder pressures. While MAG-3 renal scintigraphy may be useful in assessing drainage and differential renal function, children are often followed by serial serum creatinine and ultrasound. A nadir serum creatinine higher than 1.0 mg/dL after a period of bladder decompression indicates a higher risk of progressive deterioration in renal function as the patient ages [41].

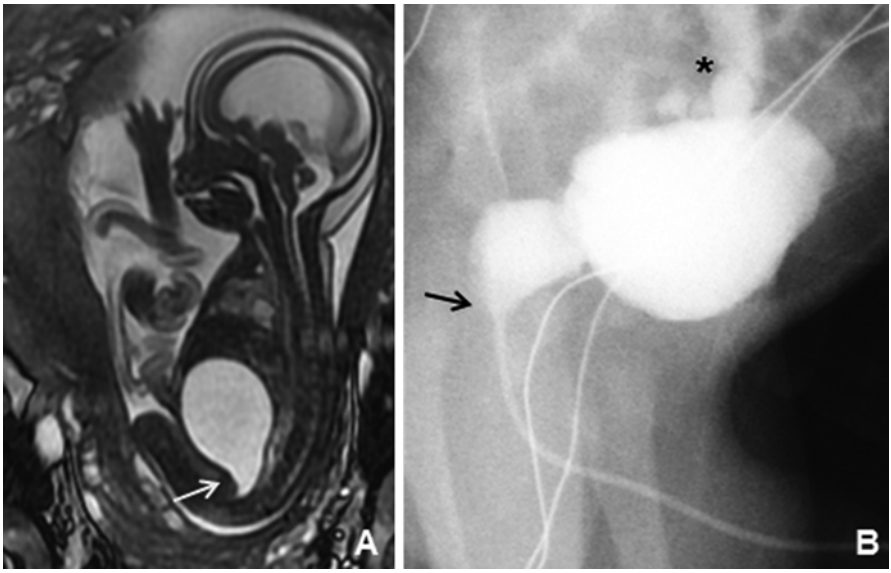

Fig. 12.16 MRI and VCUG showing PUV. (**a**) This prenatal MRI demonstrates a markedly distended bladder which is bright on T2-weighted imaging and a classic "keyhole" sign, as demonstrated by the *arrow*. (**b**) On postnatal VCUG, the posterior urethra is dilated with a distinct transition point at the area of the valve, indicated by the *arrow*. High grade reflux is also demonstrated (*asterisk*)

Prune-belly syndrome can also present with similar prenatal findings of severe bilateral hydroureteronephrosis and a distended, thick-walled bladder. The kidneys may appear hyperechoic or even cystic in severe cases. Postnatally, the posterior urethral may also be dilated in a patient with prune-belly syndrome; however the transition to the posterior urethra in prune-belly syndrome is more tapered than the abrupt transition seen with PUV. The bladder neck is often gaping and patulous due to aplasia of the prostate in prune-belly syndrome. Clinical diagnosis of prune-belly syndrome is established postnatally by the triad of deficiency of the abdominal wall musculature, bilateral non-palpable undescended testes, and an anomalous urinary tract including varying degrees of hydronephrosis, vesicoureteral reflux, renal dysplasia, dilated tortuous ureters, and an enlarged bladder.

Anterior Urethral Valve

An anterior urethral valve is a rare cause of obstruction in male infants. Much like PUV, bilateral hydronephrosis, bladder thickening, and oligohydramnios may be detected. Postnatally, patients may void with a weak stream and a midline scrotal bulge with voiding may be appreciated. In older children urinary frequency or UTI may be the presenting symptoms. VCUG will demonstrate an obstructing valve at the penoscrotal, bulbar, or penile urethra [34]. As with all cases of bladder outlet obstruction, VUR is often present. Other rare urethral anomalies such as a

dilated prostatic utricle which is commonly associated with severe hypospadias, megalourethra usually seen in prune-belly syndrome, and congenital urethral diverticulum are diagnosed with VCUG.

Summary

Imaging in the pediatric patient is critical to the diagnosis and management plan for many congenital urologic anomalies. One must be familiar with the possible conditions and various imaging modalities, including their risks and benefits as well as their limitations. Combined with a thorough history and physical exam, imaging is an invaluable adjunct to the workup of congenital genitourinary conditions.

References

1. Campbell MF, Walsh PC, Retik AB. Campbell's urology. 10th ed. Philadelphia: Saunders; 2012.
2. Hsieh MH, Lai J, Saigal CS. Trends in prenatal sonography use and subsequent urologic diagnoses and abortions in the United States. J Pediatr Urol. 2009;5:490–4.
3. Grandjean H, Larroque D, Levi S. Sensitivity of routine ultrasound screening of pregnancies in the Eurofetus database. The Eurofetus Team. Ann N Y Acad Sci. 1998;847:118–24.
4. Sty JR, Pan CG. Genitourinary imaging techniques. Pediatr Clin North Am. 2006;53:339–61.
5. Gloor JM. Management of prenatally detected fetal hydronephrosis. Mayo Clin Proc. 1995;70:145–52.
6. Cohen HL, Cooper J, Eisenberg P, et al. Normal length of fetal kidneys: sonographic study in 397 obstetric patients. Am J Roentgenol. 1991;157:545–8.
7. Lee RS, Cendron M, Kinnamon DD, et al. Antenatal hydronephrosis as a predictor of postnatal outcome: a meta-analysis. Pediatrics. 2006;118:586–93.
8. Corteville JE, Gray DL, Crane JP. Congenital hydronephrosis: correlation of fetal ultrasonographic findings with infant outcome. Am J Obstet Gynecol. 1991;165:384–8.
9. Nguyen HT, Herndon CD, Cooper C, et al. The Society for Fetal Urology consensus statement on the evaluation and management of antenatal hydronephrosis. J Pediatr Urol. 2010;6:212–31.
10. Belman AB, King LR, Kramer SA. Clinical pediatric urology. 4th ed. London: Martin Dunitz; 2002.
11. Fernbach SK, Feinstein KA, Schmidt MB. Pediatric voiding cystourethrography: a pictorial guide. Radiographics. 2000;20:155–71.
12. Goldfarb CR, Srivastava NC, Grotas AB, et al. Radionuclide imaging in urology. Urol Clin North Am. 2006;33:319–28.
13. Willi U, Treves S. Radionuclide voiding cystography. Urol Radiol. 1983;5:161–73.
14. Rushton HG, Majd M, Chandra R, Yim K. Evaluation of 99mTechnetium-dimercapto-succinic acid renal scans in experimental acute pyelonephritis in piglets. J Urol. 1988;140:1169–74.
15. Majd M, Rushton HG, Chandra R, et al. Technetium-99m-DMSA renal cortical scintigraphy to detect experimental acute pyelonephritis in piglets: comparison of planar (pinhole) and SPECT imaging. J Nucl Med. 1996;37:1731–4.
16. Ross SS, Kardos S, Krill A, et al. Observation of infants with SFU grades 3-4 hydronephrosis: worsening drainage with serial diuresis renography indicates surgical intervention and helps prevent loss of renal function. J Ped Uro. 2011;7:266–71.

17. Brant WE, Helms CA. Fundamentals of diagnostic radiology. 4th ed. Baltimore: Williams & Wilkins; 2012.
18. Caire JT, Ramus RM, Magee KP, et al. MRI of fetal genitourinary anomalies. Am J Roentgenol. 2003;181:1381–5.
19. Cerwinka WH, Grattan-Smith JD, Kirsch AJ. Magnetic resonance urography in pediatric urology. J Pediatr Urol. 2008;4:74–82.
20. Madj M, Nussbaum Blask AR, Markle BM, et al. Acute pyelonephritis: comparison of diagnosis with 99mTc-DMCA, SPECT, spiral CT, MR imaging, and power Doppler US in an experimental pig model. Radiology. 2001;218:101–8.
21. Fernbach SK, Maizels M, Conway JJ. Ultrasound grading of hydronephrosis: introduction to the system used by the Society of Fetal Urology. Pediatr Radiol. 1993;23:478.
22. Bajpai M, Chadrasekharam VV. Nonoperative management of neonatal moderate to severe bilateral hydronephrosis. J Urol. 2002;167:662–5.
23. Calaway AC, Whittam B, Szymanski KM, et al. Multicystic dysplastic kidney: is an initial voiding cystourethrogram necessary? Can J Urol. 2014;21:7510–4.
24. Avner ED, Sweeney Jr WE. Renal cystic disease: new insights for the clinician. Pediatr Clin North Am. 2006;53:889–909.
25. Chen WY, Lin CN, Chao CS, et al. Prenatal diagnosis of congenital mesoblastic nephroma in mid-trimester by sonography and magnetic resonance imaging. Prenat Diagn. 2003;23:927–31.
26. Kelner M, Droulle P, Didier F, et al. The vascular "ring" sign in mesoblastic nephroma: report of two cases. Pediatr Radiol. 2003;33:123–8.
27. Chaudry G, Perez-Atayde AR, Ngan BY, Gundogan M, Daneman A. Imaging of congenital mesoblastic nephroma with pathological correlation. Pediatr Radiol. 2009;39:1080–6.
28. Dickson PV, Sims TL, Streck CJ, et al. Avoiding misdiagnosing neuroblastoma as Wilms tumor. J Pediatr Surg. 2008;43:1159–63.
29. Naranjo A, Parisi MT, Shulkin BL, et al. Comparison of ^{123}I-metaiodobenzylguanidine (MIBG) and ^{131}I-MIBG semi-quantitative scores in predicting survival in patients with stage 4 neuroblastoma: a report from the Children's Oncology Group. Pediatr Blood Cancer. 2011;56:1041–5.
30. Lee NG, Rushton HG, Peters CA, et al. Evaluation of prenatal hydronephrosis: novel criteria for predicting vesicoureteral reflux on ultrasonography. J Urol. 2014;192:914–8.
31. Yeung CK, Godley ML, Dhillon HK, et al. The characteristics of primary vesico-ureteric reflux in male and female infants with pre-natal hydronephrosis. Br J Urol. 1997;80:319–27.
32. Martin AD, Iqbal MW, Sprague BM, et al. Most infants with dilating vesicoureteral reflux can be treated nonoperatively. J Urol. 2013;191:1620–7.
33. Skoog SJ, Peters CA, Arant BS, et al. Pediatric vesicoureteral reflux guidelines panel summary report: clinical practice guidelines for screening siblings of children with vesicoureteral reflux and neonates/infants with prenatal hydronephrosis. J Urol. 2010;184:1145–51.
34. Palmer LS. Pediatric urologic imaging. Urol Clin North Am. 2006;33:409–23.
35. Shukla AR, Cooper J, Patel RP, et al. Prenatally detected primary megaureter: a role for extended followup. J Urol. 2005;173:1353–6.
36. McLellan DL, Retik AB, Bauer SB, et al. Rate and predictors of spontaneous resolution of prenatally diagnosed primary nonrefluxing megaureter. J Urol. 2002;168:2177–80.
37. Ismaili K, Hall M, Donne C, et al. Results of systematic screening for minor degrees of fetal renal pelvis dilatation in an unselected population. Am J Obstet Gynecol. 2003;188:242–6.
38. Abuhamad AZ, Horton CE, Horton SH, et al. Renal duplication anomalies in the fetus: clues for prenatal diagnosis. Ultrasound Obstet Gynecol. 1996;7:174–7.
39. Blane CE, Zerin JM, Bloom DA. Bladder diverticula in children. Radiology. 1994;190:695–7.
40. Berrocal T, Lopez-pereira P, Arjonilla A, et al. Anomalies of the distal ureter, bladder, and urethra in children: embryologic, radiologic, and pathologic features. Radiographics. 2002;22:1139–64.
41. DeFoor W, Clark C, Jackson E, et al. Risk factors for end stage renal disease in children with posterior urethral valves. J Urol. 2008;180:1705–8.